Journal of Aerosol Science 167 (2023) 106090

Contents lists available at ScienceDirect

Journal of Aerosol Science

journal homepage: www.elsevier.com/locate/jaerosci

Hydrogen-assisted spark generation of silver nanoparticles: The effect of hydrogen content on the signal intensity in surface-enhanced Raman spectroscopy

Attila Kohut

Department of Optics and Quantum Electronics, University of Szeged, 6720 Szeged, Dóm sq. 9, Hungary

ARTICLE INFO

Keywords:
Spark ablation
Aerosol technology
Field enhancement
SERS
Hydrogen

ABSTRACT

We employed the so-called hydrogen-assisted spark generation method to produce silver nanoparticles by means of a repetitive spark discharge in a flowing gas atmosphere. Different compositions of H_2–Ar mixtures were used as carrier gas to systematically investigate the effect of the hydrogen content on the signal enhancement obtainable with silver nanoparticles in Raman spectroscopic measurements. To this end, the particles were collected on filters and used as SERS substrates without further preparation. It was shown that a ca. 50-fold signal-increase can be achieved by adding at least 30% H_2 to the Ar gas. The potential causes of the enhancement were also investigated, and they were associated partly with more pronounced aggregation on the filter and partly with the increased resilience of the silver particles against surface oxidation. The latter effect was supported by control experiments with non-oxidizable gold nanoparticles, which did not exhibit considerable enhancement-variation regardless of the hydrogen content.

1. Introduction

Spark ablation has been proven to be a convenient, versatile, and scalable method for the generation of non-insulating nanoparticles (NPs) in the gas phase (Schmidt-Ott, 2020). Since spark discharge nanoparticle generators (SDGs) are based on the periodic ablation of a pair of electrodes in a regulated gaseous environment, the purity of the produced particles can strictly be controlled. Hence, due to the absence of various solvents and reagents, exceptionally pure NPs can form (Lehtinen, Backman, Jokiniemi, & Kulmala, 2004). Even though, both bulk electrode materials and carrier gases are available in high purity form, the introduction of a trace amount of oxygen to the system is inevitable (Seipenbusch, Weber, Schiel, & Kasper, 2003). Depending on the reactivity of the electrode material this can lead to oxide formation, which is undesirable in some applications. In most physical vapor deposition processes, oxygen is removed from the synthesis volume via maintaining ultra-high vacuum (Llamosa et al., 2014), which is obviously not viable during spark ablation, which takes place at atmospheric pressure in a flowing gas. Inhibiting the oxidation in an SDG is feasible via employing rigorous gas purification, outgassing, and sample treatment steps as demonstrated by Vons et al. during the production of unoxidized magnesium and silicon NPs (Vons, Anastasopol, et al., 2011; Vons, De Smet et al., 2011). This approach, however, makes the process highly complicated and hence cannot realistically be employed for general purposes on a regular basis. To overcome the issue of oxidation, Hallberg et al. have proposed the addition of hydrogen to the carrier gas, acting as a reducing agent during the particle formation process (Hallberg et al., 2018). They have demonstrated that as small as five volumetric percent of hydrogen in the carrier gas not only facilitates the more complete compaction of NP aggregates (Olszok, Bierwirth, & Weber, 2021;

E-mail address: kohut.attila@szte.hu.

https://doi.org/10.1016/j.jaerosci.2022.106090
Received 5 July 2022; Received in revised form 15 September 2022; Accepted 23 September 2022
Available online 28 September 2022

Seipenbusch et al., 2003), but significantly reduces the formation of oxide primary particles in case of non-noble metals as well. Thus, as it was further shown by the same research group, the addition of hydrogen to the carrier gas during particle generation is an appealingly simple approach to control the oxidation and self-passivation of aerosol NPs (Preger et al., 2019). In addition to increasing the resistance to oxidation of the generated particles during ambient storage (Snellman, Eom, Ek, Messing, & Deppert, 2021), the presence of hydrogen seems to have an important role in the formation of multielement, crystalline alloys of unconventional material-combinations as well (Feng et al., 2020). Even though, the significance of a hydrogen-containing carrier gas has been emphasized mostly in the context of aerosol-based synthesis of non-noble metals so far, in certain contexts, it can also be relevant for metals less prone to oxidation. A prominent example is the electrical field enhancement experienced in the vicinity of nanostructures or nanostructured surfaces due to the effect of localized surface plasmons (Willets & Van Duyne, 2007) exploited, for instance, in surface-enhanced Raman spectroscopy (SERS) (Langer et al., 2019). The conditions for resonant excitation of surface plasmons, and hence for maximum signal enhancement, can be achieved by employing certain materials, all of which gold and silver are the most widely used (Pilot et al., 2019). Silver is of particular interest in many applications due to its remarkable enhancement, however, it is known to form a thin surface oxide layer, which has a considerable effect on its performance (Pilot et al., 2019). This might even be more important in silver-based SERS substrate fabrication methods employing aerosol routes in the absence of protective and stabilizing agents. A premier example to such aerosol approach is spark ablation, which was shown to have great potential in the fabrication of SERS substrates from various materials, including Au, Ag, Cu and their alloys on various substrate types, such as silicon wafer, microfiber filters, optical fibers, or even dye films (El-Aal, Seto, Kumita, Abdelaziz, & Otani, 2018, 2020; El-Aal & Seto, 2021; Ivanov et al., 2022; Kohut et al., 2020; Kohut, Horváth, et al., 2021). In the present study, we employed hydrogen-assisted spark generation to synthesize silver NPs and deposited them onto PVDF (polyvinylidene fluoride) filters directly from the aerosol phase. The silver-loaded filters were employed as SERS-substrates for measuring the Raman signal of a test analyte. The signal-enhancement achieved by the fabricated substrates was investigated as a function of the hydrogen content of the carrier gas. After considering and investigating potential concomitant effects on the measured Raman intensity, it can be concluded that the presence of hydrogen at spark-generation of silver NPs has a considerable beneficial effect on their SERS-performance.

2. Material and methods

The experimental setup used in the present study was previously described in detail (Kohut et al., 2020; Kohut, Villy, et al., 2021), therefore here we only give a brief overview of the most important aspects. NP generation was carried out by using a custom-made SDG employing a monolithic, high voltage 8 nF capacitor (50PM980, General Atomics Inc) and a high voltage capacitor charger power supply (HCK 800–12500, FuG GmbH). The total inductance and resistance of the discharge circuit is ca. 1 μH and 1 Ω, respectively. The sparking was maintained inside a gas-tight stainless-steel chamber between a pair of cylindrical, 3 mm diameter electrodes, with a 2.0 mm interelectrode distance. Ag (99.9% purity, Goodfellow Cambridge Ltd) and Au (99.9% purity, Goodfellow Cambridge Ltd) were used as electrode materials. The spark repetition rate was kept constant at 100 Hz in all experiments. Different mixtures of argon (99.996% purity, Messer Hungarogáz Kft.) and hydrogen (99.999% purity, Messer Hungarogáz Kft.) was employed as carrier gas, entering the chamber from below via an upward pointing inlet tube of 3 mm inner diameter, 5 mm away from the electrodes' common axis (in a so-called upward pointing "cross-flow" geometry). The total gas flow rate was kept at 5.0 L/min, controlled by two separate mass flow controllers for Ar and H_2 (GFC16 and GFC15, respectively, Aalborg Inc.). All experiments were carried out at 1100 mbar pressure. Heat treatment of the as-formed NP aggregates was carried out by passing the aerosol leaving the SDG chamber through a tube furnace (EHA 12/300B, Carbolite Gero GmbH.) set to a constant temperature of 800 °C. The residence time inside the furnace is estimated to be ca. 12 s. The generated particles were collected on PVDF filters (HVLP04700, Merck KGaA, 47 mm diameter) by using a stainless-steel filter house (XX4404700, Millipore Corp.). In most of the experiments the deposition time was kept constant at 10 min, unless stated otherwise in the text.

The total concentration of the generated NPs was measured – after dilution of the aerosol – by using a condensation particle counter (Model 3756, TSI Inc.). Morphology of the NPs was investigated by transmission electron microscopy (Tecnai G2 20 X-TWIN HR-TEM, Thermo Fisher Scientific Inc.), after sampling on TEM grids (Lacey Carbon Films on 200 Mesh Copper Grids, Agar Scientific Ltd.) by means of a low-pressure inertial impactor. Extinction spectra of the NP-loaded filters were measured by using a modified optical microscope (Labophot-2, Nikon Corp.) in transmission mode equipped with an off-axis parabolic mirror (RC12SMA-P01, Thorlabs Inc.) for light collection and a compact spectrometer (AvaSpec-ULS3648, Avantes BV) for spectral analysis. Filters without nanostructure were used to acquire reference spectra. SERS performance of the NP-loaded filters was assessed without further treatment by measuring the Raman spectrum of Rhodamine 6G (R6G, Fluka AG) solution in ethanol, dripped and dried onto the filter in ambient air. Rhodamine 6G concentrations of 1 mM and 100 mM were used in measurements with and without NPs, respectively. Raman spectra were obtained by using a Raman microscope (DXR, Thermo Fisher Scientific Inc.) at an excitation wavelength of 780 nm.

3. Results and discussion

In order to investigate the potential effects of a hydrogen-containing carrier gas on the SERS performance of spark-generated Ag NPs, the produced particles were collected on PVDF filters, which were employed as SERS substrates without any pre- or post-treatment. The application of filters facilitated a well-controlled, constant sampling of the generated particles, without introducing additional variables related to substrate fabrication. It is important to note, however, that the present study does not aim for achieving the highest enhancement factors or lowest limit of detections possible, therefore the substrates were not optimized in this sense. Nevertheless, the obtained enhancement factors were sufficient at every experimental condition to facilitate a systematic assessment of

the variations associated with the addition of hydrogen to the carrier gas of the SDG. As it is shown in Fig. 1A, the effect of hydrogen on the intensity of the analyte's Raman spectrum is evident. The Ag NPs generated in a pure Ar environment resulted in a ca. 100-times signal increase as compared to the reference spectrum obtained without NPs on the filter, which then further increases by about an order of magnitude when the carrier gas flow contains 5% hydrogen. To interpret these results, further properties of spark-ablation must be taken into account. First of all, the variation of the discharge voltage has to be considered, associated with the higher breakdown voltage of hydrogen as compared to argon (Christophorou, Olthoff, & Green, 1997). By introducing 5% hydrogen to the carrier gas, the discharge voltage increases by ca. 20% (from 2.50 ± 0.01 kV to 2.99 ± 0.02 kV) resulting in about 44% more energy stored in the capacitor of the SDG, which is fed into the spark gap. It should be noted that the relation between the energy stored in the capacitor and the actual spark energy is rather nontrivial, nevertheless it is broadly accepted that it affects the primary particle size (Feng et al., 2016) and the total concentration of the generated particles as well (Tabrizi, Ullmann, Vons, Lafont, & Schmidt-Ott, 2009). As can be seen in Fig. 1C and D, there is only a slight increase in the modal diameter of the generated particles. The modus increases from 7.2 nm to 7.6 nm, when 5% of hydrogen is added to the carrier gas. Such a minor difference is not expected to have an as major impact on the enhancement factor, as seen in Fig. 1A. By looking at the variation of the total concentration of the generated particles, a somewhat higher, ca. 10% increase can be observed. Due to the constant sampling time, this means that the particle loading in the filter also increases. As shown in Fig. 1B, a considerably higher peak extinction is associated to the hydrogen-containing scenario with a negligible shift in its position. Such a great variation in the extinction spectrum cannot be solely explained by the higher particle loading, as shown by the reference curve (dashed black curve) included in Fig. 1B. This curve represents a case when no hydrogen was present, but the particle loading of the filter was increased by 10% via using 10% longer collection time. Fig. 1B suggests that the presence of hydrogen has further effects on the generated Ag NPs in addition to the increased particle loading.

In order to further investigate the effect of hydrogen in the carrier gas on the SERS performance of the spark-generated Ag NPs, we fabricated filter-based substrates at systematically increasing H_2 content and measured the corresponding enhancement factors. The EF was calculated by using the well-known formula (Yu & White, 2012):

$$EF = \frac{I_{SERS}}{I_{Raman}} \frac{N_{Raman}}{N_{SERS}}$$

where I_{SERS} and I_{Raman} represent the intensity of a selected line (here the one at 1506 cm^{-1}) with and without the presence of nanoparticles, respectively. While N_{SERS} and N_{Raman} denote the number of analyte molecules excited in the corresponding cases. Due to the structure of the filters used as support for the particles, we assumed that the number of analyte molecules in the excited area is proportional to the concentration of the analyte in solution, therefore the number ratio can be replaced by the concentration ratio in the above formula.

The variation of the EF as a function of the H_2 content in the carrier gas is shown in Fig. 2A. It can be seen that the EF increases quasi linearly with increasing hydrogen content up to 30%, when reaches a plateau. At this plateau, the EF is ca. 50-times higher than that is in pure argon, which is a considerable increase, associated with the application of hydrogen in the carrier gas.

As it was previously pointed out, the presence of hydrogen in the SDG chamber has an effect on the spark energy. As shown in

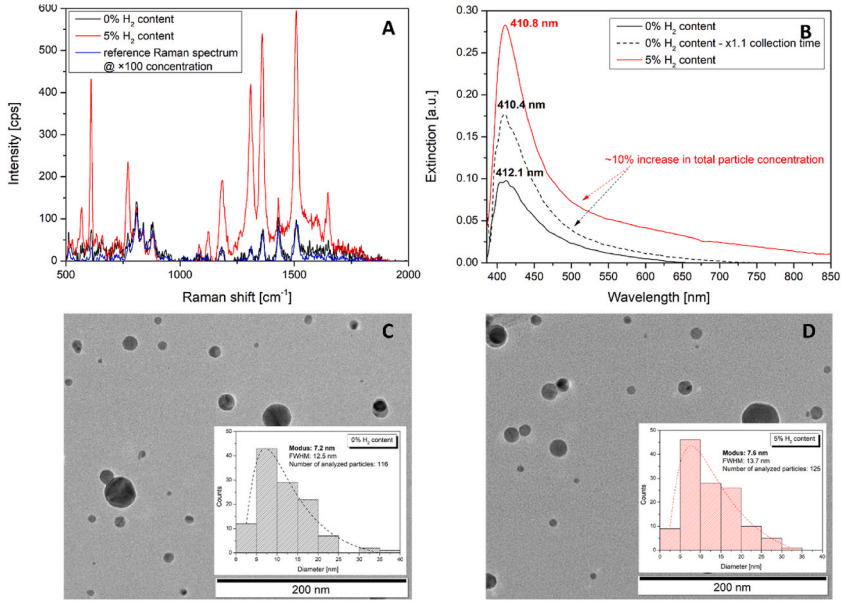

Fig. 1. The Raman spectrum of the analyte measured on a reference filter without nanoparticles, and on Ag-loaded filters with and without adding H_2 to the Ar carrier gas (**A**). The extinction spectra of the Ag-loaded filters at different H_2 contents (**B**). TEM micrograph of the generated Ag NPs with the corresponding size distribution at 0% (**C**) and 5% (**D**) H_2 content in the carrier gas.

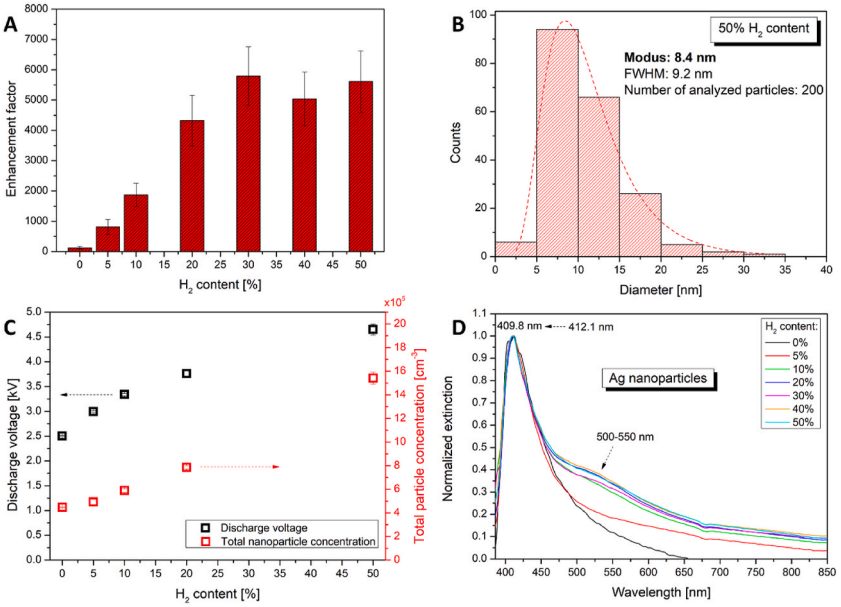

Fig. 2. Variation of the enhancement factor of Ag NP-loaded filters used as SERS substrates fabricated at varying H_2 content of the carrier gas (**A**). Size distribution of Ag NPs produced at 50% H_2 content (**B**). Variation of the discharge voltage and the total particle concentration as a function of the H_2 content of the carrier gas (**C**). Extinction spectra of Ag NP-loaded filters, generated at varying H_2 content (**D**).

Fig. 2C, the discharge voltage monotonously increases with increasing hydrogen content, which in turn increases the total number concentration of the generated NPs. A slight shift in the modus of the particle size distribution can also be observed in Fig. 2B (from 7.6 nm to 8.4 nm when increasing the H_2 content from 5% to 50%), but it is much less pronounced than that of the concentration-increase. Due to the increasing total concentration and the fixed collection time, the particle loading in the filters also increases, which gives rise to aggregation leading to the formation of so-called hot spots, which are known to have much more significant contribution to the total field enhancement than that of the separate NPs (Mosier-Boss, 2017). The appearance of a broad spectral feature around 500–550 nm in the extinction spectra of the NP-loaded filters, shown in Fig. 2D, is a sign of aggregation, hence supports the above idea.

As an attempt to decouple the effect of increased particle loading and hence the aggregate formation from the effect of the presence of hydrogen, Ag NPs were generated in pure Ar and collected on filters with increasing collection times. These periods were adjusted by using the total concentration values shown in Fig. 2C to achieve similar particle loadings as obtained during the application of H_2. The

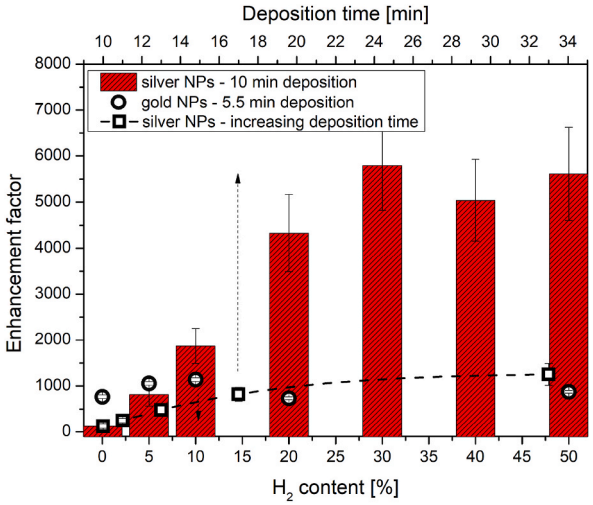

Fig. 3. Enhancement factor of silver (columns) and gold (empty circles) NPs as a function of the hydrogen content of the carrier gas (bottom horizontal axis). Enhancement factor of silver NPs (empty squares) produced in pure Ar as a function of deposition time (top horizontal axis). The points are connected to guide the eyes only. (For interpretation of the references to colour in this figure legend, the reader is referred to the Web version of this article.)

SERS activity of these substrates were tested and compared to the filters loaded with Ag NPs prepared under H_2-containing atmosphere. The enhancement factors obtained for both set of measurements are plotted together in Fig. 3. It can be seen that the EF indeed increases with increasing deposition time – just as expected considering the effect of aggregation – but with a smaller extent than that is associated with the application of hydrogen. This proves that a hydrogen-containing carrier gas does have a beneficial effect on the enhancement factor of Ag NPs produced in the SDG. It should also be noted that the extinction spectra shown in Fig. 2D indicate that the level of aggregation does not vary significantly above ca. 10% H_2 content. However, the EF still increases considerably (by a factor of ca. 3), when the hydrogen content is increased further from 10 to 30%. This also indicates the beneficial effect of hydrogen on the SERS performance of silver nanoparticles beyond the improved aggregation.

Even though silver is generally considered to be a precious metal and it is less prone to oxidation, it has a tendency to form a surface oxide layer. This has a well-known deteriorating effect on the activity of silver-based SERS substrates (Pilot et al., 2019). Han et al. attempted to quantify this effect and obtained a steeply dropping EF as a function of the thickness of the Ag_2O layer on the particle surface, indicating a ca. three orders of magnitude decrease at sub-monolayer thicknesses (Han et al., 2011). This points out that even a slight variation of the oxide layer thickness can have a substantial effect on the SERS signal. Silver oxide, however, is known to thermally decompose to silver and oxygen at temperatures above ca. 400 C° (Waterhouse, Bowmaker, & Metson, 2001), which is below the compaction temperature used in the present study. Therefore, it can be assumed that, even without hydrogen, the compacted, spherical particles obtained after the tube furnace are pure silver and oxidation can occur later during deposition and ambient handling and storage. As it was shown by Matikainen et al., oxygen content of silver nanoparticles quickly builds up under ambient conditions resulting in a ca. one order of magnitude drop of the SERS intensity in less than 24 h (Matikainen et al., 2016). Our observations indicate that the presence of hydrogen in the SDG during particle generation and compaction helps – at least partially – reducing the thickness of the oxide layer forming on the surface of the Ag NPs collected on the filters. Such a "protective" effect of the hydrogen is in line with the observations of other authors reporting prolonged resilience of other metal nanoparticles to oxidation during ambient storage (Feng et al., 2020; Snellman et al., 2021). To provide further evidence that the increase in SERS signal intensity observed during the application of H_2 is related to oxidation, gold NPs were fabricated as a non-oxidizable reference material. The Au NPs were produced at varying the hydrogen-content of the carrier gas and collected on filters. For keeping the particle loading on the filters similar to that of the Ag NPs, the deposition time was adjusted according to the total concentration. As can be seen in Fig. 3 there is no systematic variation in the EF, irrespectively from the H_2 content. The EF scatters around the ca. 1000 value both at 0% and 50% hydrogen, showing that the presence of hydrogen doesn't affect the SERS performance of the NP-loaded filters when a non-oxidizable material is used. This result also points to the oxidation of the Ag NPs as the main effect, which is being reduced by applying H_2 in the carrier gas.

4. Conclusions

We have employed the so-called hydrogen-assisted spark generation method to produce silver nanoparticles in the gas phase while systematically varying the hydrogen content of the Ar–H_2 carrier gas. After collecting the generated particles on PVDF filters, surface-enhanced Raman spectroscopic measurements were carried out on an analyte dripped and dried on the surface of the filters. The effect of the hydrogen content of the carrier gas on the Raman signal enhancement was assessed. Using 30% or more H_2 resulted in a ca. 50-times increase in the enhancement factor exhibited by the Ag nanoparticle-loaded filters. It was shown that a part of this enhancement (ca. 10-fold) is due to the increased particle concentration, which causes more pronounced aggregation and hence hot-spot formation for more effective electric field enhancement. On the top of this effect, the presence of hydrogen causes an additional 5-fold signal increase, which is most probably associated with the reduction of the surface oxide layer tend to form on silver particles during and after deposition. This explanation was strengthened by results obtained with non-oxidizable gold nanoparticles, which did not cause considerable Raman signal variation regardless of the hydrogen content. Our findings help emphasizing the benefits of the hydrogen-assisted spark generation method even in cases where complete oxidation is not necessarily an issue, but surface-dependent applications of the produced particles are aimed.

Declaration of competing interest

The authors declare that they have no known competing financial interests or personal relationships that could have appeared to influence the work reported in this paper.

Data availability

Data will be made available on request.

Acknowledgments

We are grateful for the Ministry of Innovation and Technology of Hungary for the funding provided from the National Research, Development and Innovation Fund under the PD_21 OTKA funding scheme (PD 139077 project). Research leading to these results has also received funding from the GINOP-2.3.2-15-2016-00036 as well as the TUDFO/47138–1/2019-ITM and TKP2021-NVA-19 projects.

References

Christophorou, L. G., Olthoff, J. K., & Green, D. S. (1997). Gases for electrical insulation and arc interruption: Possible present and future alternatives to pure SF6. *NIST Technical Note, 1425*, 48.

El-Aal, M. A., & Seto, T. (2021). Spark discharge deposition of au/cu nanoparticles for surface-enhanced Raman scattering. *Surface and Interface Analysis, 53*(9), 824–828. https://doi.org/10.1002/sia.6975

El-Aal, M. A., Seto, T., Kumita, M., Abdelaziz, A. A., & Otani, Y. (2018). Synthesis of silver nanoparticles film by spark discharge deposition for surface-enhanced Raman scattering. *Optical Materials, 83*, 263–271. https://doi.org/10.1016/j.optmat.2018.06.029

El-Aal, M. A., Seto, T., & Matsuki, · A. (2020). The effects of operating parameters on the morphology, and the SERS of Cu NPs prepared by spark discharge deposition. *Applied Physics A, 126*, 572. https://doi.org/10.1007/s00339-020-03762-5

Feng, J., Chen, D., Pikhitsa, P.v., Jung, Y. ho, Yang, J., & Choi, M. (2020). Unconventional alloys confined in nanoparticles: Building blocks for new matter. *Matter, 3*(5), 1646–1663. https://doi.org/10.1016/j.matt.2020.07.027

Feng, J., Huang, L., Ludvigsson, L., Messing, M. E., Maisser, A., Biskos, G., et al. (2016). General approach to the evolution of singlet nanoparticles from a rapidly quenched point source. *Journal of Physical Chemistry C, 120*(1), 621–630. https://doi.org/10.1021/acs.jpcc.5b06503

Hallberg, R. T., Ludvigsson, L., Preger, C., Meuller, B. O., Dick, K. A., & Messing, M. E. (2018). Hydrogen-assisted spark discharge generated metal nanoparticles to prevent oxide formation. *Aerosol Science and Technology, 52*(3), 347–358. https://doi.org/10.1080/02786826.2017.1411580

Han, Y., Lupitskyy, R., Chou, T.-M., Stafford, C. M., Du, H., & Sukhishvili, S. (2011). Effect of oxidation on surface-enhanced Raman scattering activity of silver nanoparticles: A quantitative correlation. *Anal. Chem, 83*, 5873. https://doi.org/10.1021/ac2005839

Ivanov, V., Lizunova, A., Rodionova, O., Kostrov, A., Kornyushin, D., Aybush, A., et al. (2022). Aerosol dry printing for SERS and photoluminescence-active gold nanostructures preparation for detection of traces in dye mixtures. *Nanomaterials, 12*(3), 448. https://doi.org/10.3390/NANO12030448

Kohut, A., Horváth, V., Pápa, Z., Vajda, B., Kopniczky, J., Galbács, G., et al. (2021). One-step fabrication of fiber optic SERS sensors via spark ablation. *Nanotechnology, 32*(29), Article 395501. https://doi.org/10.1088/1361-6528/ac0c41

Kohut, A., Kéri, A., Horváth, V., Kopniczky, J., Ajtai, T., Hopp, B., et al. (2020). Facile and versatile substrate fabrication for surface enhanced Raman spectroscopy using spark discharge generation of Au/Ag nanoparticles. *Applied Surface Science, 531*, Article 147268. https://doi.org/10.1016/j.apsusc.2020.147268

Kohut, A., Villy, L. P., Kéri, A., Bélteki, Á., Megyeri, D., Hopp, B., et al. (2021). Full range tuning of the composition of Au/Ag binary nanoparticles by spark discharge generation. *Scientific Reports, 11*(1), 5117. https://doi.org/10.1038/s41598-021-84392-6

Langer, J., Jimenez De Aberasturi, D., Aizpurua, J., Alvarez-Puebla, R. A., Auguié, B., Baumberg, J. J., et al. (2019). Present and future of surface-enhanced Raman scattering. *ACS Nano, 14*(1), 28–117. https://doi.org/10.1021/acsnano.9b04224

Lehtinen, K. E. J., Backman, U., Jokiniemi, J. K., & Kulmala, M. (2004). Three-body collisions as a particle formation mechanism in silver nanoparticle synthesis. *Journal of Colloid and Interface Science, 274*, 526–530. https://doi.org/10.1016/j.jcis.2004.01.023

Llamosa, D., Ruano, M., Martínez, L., Mayoral, A., Roman, E., García-Hernández, M., et al. (2014). The ultimate step towards a tailored engineering of core@shell and core@shell@shell nanoparticles. *Nanoscale, 6*(22), 13483–13486. https://doi.org/10.1039/c4nr02913e

Matikainen, A., Nuutinen, T., Itkonen, T., et al. (2016). Atmospheric oxidation and carbon contamination of silver and its effect on surface-enhanced Raman spectroscopy (SERS). *Scientific Reports, 6*, Article 37192. https://doi.org/10.1038/srep37192

Mosier-Boss, P. (2017). Review of SERS substrates for chemical sensing. *Nanomaterials, 7*(6), 142. https://doi.org/10.3390/nano7060142

Olszok, V., Bierwirth, M., & Weber, A. P. (2021). Interaction of reactive gases with platinum aerosol particles at room temperature: Effects on morphology and surface properties. *Nanomaterials, 11*, 2266. https://doi.org/10.3390/nano11092266

Pilot, R., Signorini, R., Durante, C., Orian, L., Bhamidipati, M., & Fabris, L. (2019). A review on surface-enhanced Raman scattering. *Biosensors, 9*(2), 57. https://doi.org/10.3390/bios9020057

Preger, C., Bulbucan, C., Meuller, B. O., Ludvigsson, L., Kostanyan, A., Muntwiler, M., et al. (2019). Controlled oxidation and self-passivation of bimetallic magnetic FeCr and FeMn aerosol nanoparticles. *Journal of Physical Chemistry C, 123*(26), 16083–16090. https://doi.org/10.1021/acs.jpcc.9b01678

Schmidt-Ott. (2020). In Andreas (Ed.), *Spark ablation: Building blocks for nanotechnology*. Jenny Stanford Publishing.

Seipenbusch, M., Weber, A. P., Schiel, A., & Kasper, G. (2003). Influence of the gas atmosphere on restructuring and sintering kinetics of nickel and platinum aerosol nanoparticle agglomerates. *Journal of Aerosol Science, 34*(12), 1699–1709. https://doi.org/10.1016/S0021-8502(03)00355-0

Snellman, M., Eom, N., Ek, M., Messing, M. E., & Deppert, K. (2021). Continuous gas-phase synthesis of core-shell nanoparticlesviasurface segregation. *Nanoscale Advances, 3*(11), 3041–3052. https://doi.org/10.1039/d0na01061h

Tabrizi, N. S., Ullmann, M., Vons, V. A., Lafont, U., & Schmidt-Ott, A. (2009). Generation of nanoparticles by spark discharge. *Journal of Nanoparticle Research, 11*(2), 315–332. https://doi.org/10.1007/s11051-008-9407-y

Vons, V. A., Anastasopol, A., Legerstee, W. J., Mulder, F. M., Eijt, S. W. H., & Schmidt-Ott, A. (2011). Low-temperature hydrogen desorption and the structural properties of spark discharge generated Mg nanoparticles. *Acta Materialia, 59*(8), 3070–3080. https://doi.org/10.1016/J.ACTAMAT.2011.01.047

Vons, V. A., De Smet, L. C. P. M., Munao, D., Evirgen, A., Kelder, E. M., & Schmidt-Ott, A. (2011). Silicon nanoparticles produced by spark discharge. *Journal of Nanoparticle Research, 13*(10), 4867–4879. https://doi.org/10.1007/s11051-011-0466-0

Waterhouse, G. I. N., Bowmaker, G. A., & Metson, J. B. (2001). The thermal decomposition of silver (I, III) oxide: A combined xrd, FT-IR and Raman spectroscopic study. *Physical Chemistry Chemical Physics, 3*(17), 3838–3845. https://doi.org/10.1039/B103226G

Willets, K. A., & Van Duyne, R. P. (2007). Localized surface plasmon resonance spectroscopy and sensing. *Annual Review of Physical Chemistry, 58*, 267–297. https://doi.org/10.1146/ANNUREV.PHYSCHEM.58.032806.104607

Yu, W. W., & White, I. M. (2012). A simple filter-based approach to surface enhanced Raman spectroscopy for trace chemical detection. *Analyst, 137*(5), 1168–1173. https://doi.org/10.1039/c2an15947c